Correlation and relativistic effects for the 4f-nl and 5p-nl multipole transitions in Er-like tungsten

U. I. Safronova and A. S. Safronova

Phys. Rev. A **84**, 012511 — Published 22 July 2011

DOI: 10.1103/PhysRevA.84.012511

Correlation and relativistic effects for the $4f - nl$ and $5p - nl$ multipole transitions in Er-like tungsten

U. I. Safronova and A. S. Safronova
Physics Department, University of Nevada, Reno, Nevada 89557

Wavelengths, transition rates, and line strengths are calculated for the multipole (E1, M1, E2, M2, and E3) transitions between the excited [Cd]$4f^{13}5p^6nl$, [Cd]$4f^{14}5p^5nl$ configurations and the ground [Cd]$4f^{14}5p^6$ state in Er-like W^{6+} ion ([Cd]=[Kr]$4d^{10}5s^2$). In particular, the relativistic many-body perturbation theory (RMBPT), including the Breit interaction, is used to evaluate energies and transition rates for multipole transitions in this hole-particle system. This method is based on the relativistic many-body perturbation theory that agrees with MCDF calculations in lowest-order, includes all second-order correlation corrections and corrections from negative-energy states. The calculations start from a [Cd]$4d^{14}5p^6$ Dirac-Fock (DF) potential. First-order perturbation theory is used to obtain intermediate-coupling coefficients, and second-order RMBPT is used to determine the multipole matrix elements needed for calculations of other atomic properties such as line strengths and transition rates. In addition, core multipole polarizability is evaluated in random-phase and DF approximations. These are the first *ab initio* calculations of energies and transition rates in ER-like tungsten. The comparison with available data is demonstrated.

PACS numbers: 31.15.A-,31.15.am,31.15.vj,31.15.ap

I. INTRODUCTION

Correlation and relativistic effects for the $4f - nl$ multipole transitions in Er-like Yb^{2+} ion were recently studied in Ref. [1]. Specifically, the relativistic many-body perturbation theory (RMBPT) was used to evaluate wavelengths, transition rates, and line strengths for the multipole transitions between the excited [Xe]$4f^{13}ns$, [Xe]$4f^{13}nd$, and [Xe]$4f^{13}np$ and the ground [Xe]$4f^{14}$ state in Yb III ion with the nuclear charge $Z = 70$ ([Xe]=[Ni]$4s^24p^64d^{10}5s^25p^6$) [1]. The first measurement of Er-like Yb^{2+} wavelengths was reported more than forty years ago by Bryant [2] where the resonance transition array $4f^{14} - 4f^{13}5d$ was observed. All 41 energy levels (28 odd and 13 even) belonging to the $4f^{14}$, $4f^{13}5d$, $4f^{13}6s$, $4f^{13}6p$, and $4f^{13}7s$ configurations of Yb III were determined experimentally [2]. Some years later, the spectra of Er-like Lu^{3+}, Hf^{4+}, and Ta^{5+} were investigated [3–5]. The resonance transition array $4f^{14} - 4f^{13}5d$ was observed in the isoelectronic sequence from Lu IV through Ta VI. The new resonance group, corresponding to the $5p^6 - 5p^55d$ and $5p^6 - 5p^55d$ transitions, was discovered by Kaufman and Sugar [5] in Ta VI ion. Both types of resonance lines in Er-like W^{6+} were reported by Sugar and Kaufman in [6]. It was suggested [6] that the [Cd]$4f^{13}5p^6$ and [Cd]$4f^{14}5p^5$ ([Cd]=$1s^22s^22p^63s^23p^63d^{10}4s^24p^64d^{10}5s^2$) core states overlap in Er-like W^{6+} where the binding energies of the $4f_j$ and $5p_j$ orbits are nearly equal.

In Fig. 1, we plot the binding energies of the $4f_j$, $5p_j$, and $5s_{1/2}$ orbitals calculated in Dirac-Fock (DF) approximation as function of nuclear charge Z. For better presentation, we scaled those energies by a factor of $(Z - 60)^2$. We find that the $4f_{5/2}$ and $4f_{7/2}$ orbitals are more tightly bound than the $5p_j$ and $5s_{1/2}$ orbitals at low stages of ionization (Z = 72-74 for $5p_j$ and Z = 79-80 for $5s_{1/2}$), while the $5p_j$ and $5s_{1/2}$ orbitals are more tightly bound than the $4f_{5/2}$ and $4f_{7/2}$ orbitals for highly ionized cases. Near crossing of the curves describing the $4f_j$, and $5p_j$ binding energies around Z=74 leads to certain challenges in the calculations, making it difficult to obtain very accurate excitation energies and line strengths for the transitions including the $4f_j$ and $5p_j$ orbitals.

In Fig. 2, we plot the valence energies of the $5d_j$, $6p_j$, and $6s_{1/2}$ orbitals calculated in Dirac-Fock (DF) approximation as function of nuclear charge Z. We use the same scaling factor as in the Fig. 1. The ranges of energies ([0 - 8000] and [0 - 5000] in units of $(Z - 60)^2$ cm^{-1}) are similar in both figures, while the sign of the binding and valence energies are different.

In present paper, we consider the [Cd]$4f^{13}5p^6nl$ and [Cd]$4f^{14}5p^5nl$ configurations with including both $4f_j$ and $5p_j$ orbitals. We evaluate the wavelengths, transition rates, and line strengths for the multipole (E1, M1, E2, M2, and E3) transitions between the excited [Cd]$4f^{13}5p^6nl$ and [Cd]$4f^{14}5p^5nl$ configurations and the ground [Cd]$4f^{14}5p^6$ state in Er-like W^{6+} ion. We use the RMBPT code that is based on the relativistic many-body perturbation theory, that mostly agrees with MCDF calculations in lowest-order, includes all second-order correlation corrections, and includes corrections from negative-energy states.

We have utilized the RMBPT code before to evaluate the wavelengths, radiative transition rates and autoionizing rates for other tungsten ions in Refs. [7–12]. In particular, wavelengths and transition rates for $nl - n'l'$ transitions in Be-, B-, Mg-, Al-, Ca-, Zn-, Ag- and Yb-like tungsten ions were tabulated in Ref. [7]. Energies of the [Kr]$4d^94f^2$, [Kr]$4d^94f5l$, and [Kr]$4d^95l5l'$ states (with $l = s, p, d, f$) for Ag-like ions with Z = 50 - 100 were evaluated to second order RMBPT starting from a Pd-like Dirac-Fock potential, [Kr]$4d^{10}$ [8]. Energy levels, radiative matrix elements, and autoionization rates for $1s2l2l'$ states of lithiumlike Mo^{39+}, Pr^{56+}, W^{71+}, and

Hg^{77+} were evaluated in [9]. Excitation energies, radiative and autoionization rates, dielectronic satellite lines, and dielectronic recombination rates for excited states of Na-like W from Ne-like W were calculated in [10]. The same approach was used in Refs. [11, 12] to evaluate atomic properties of Mg-like W and Ag-like W excited states.

The probabilities of the $4f^{13}6p-4f^{13}5d$ electric-dipole transitions and the lifetimes of the $4f^{13}6p$ and $4f^{13}5d$ states were calculated for Yb III, Lu IV, Hf V, and Ta VI of the erbium isoelectronic sequence by Loginov and Tuchkin [13]. The wavefunctions in the intermediate coupling scheme, necessary for calculating the relative line strengths, were obtained semiempirically from experimentally measured energy intervals between fine-structure levels [13]. The same approach was used in Ref. [14] to evaluate the probabilities of the $4f^{13}6p-4f^{13}6s$ and $4f^{13}6p-4f^{13}7s$ electric-dipole transitions.

A compilation and critical review of the measured excitation energies and wavelengths in Er-like W VII was recently presented by Kramida and Shirai [15]. There has been great renewed interest in the spectral emission of tungsten from magnetically confined high-temperature plasmas [16–29]. The possibility of using extreme ultraviolet emission from low-charge states of tungsten ions to diagnose the divertor plasmas of the ITER tokamak was investigated by Clementson *et al.* [16]. Spectral modelling of Lu-like W^{3+} to Gd-like W^{10+} was performed by using the Flexible Atomic Code (FAC), and spectroscopic measurements were conducted at the Sustained Spheromak Physics Experiment (SSPX) in Livermore [16]. The electric quadrupole (E2) and magnetic octupole (M3) ground-state transitions in Ni-like W^{46+} were measured using high-resolution crystal spectroscopy at the LLNL electron-beam ion trap facility [17]. Tungsten spectra recorded at the Large Helical Device (LHD) and comparison with calculations were presented by Harte *et al.* [19]. The extreme ultraviolet (EUV) spectra from highly-charged tungsten ions in low-density and high-temperature plasmas produced in the LHD at the National Institute for Fusion Science were measured. Calculations were performed with the Hartree-Fock with CI suite of codes written by Cowan [30].

In the present paper, RMBPT is used for systematic study of atomic transitions in Er-like W^{6+} ion. Specifically, we determine energies of the $4f^{13}5p^6nl$ and $4f^{14}5p^5nl$ excited states with $nl = 5d, 6d, 6s, 7s, 5f, 6p$. The calculations are carried out to second order in perturbation theory. RMBPT is also used to determine line strengths, oscillator strengths, and transition rates for all allowed and forbidden electric-multipole and magnetic-multipole (E1, E2, E3, M1, M2) transitions from the $4f^{13}5p^6nl$ and $4f^{14}5p^5nl$ excited states into the $4f^{14}5p^6$ ground state.

As was mentioned above, this work is motivated in part by renewed interest in the spectral emission of tungsten from magnetically confined high-temperature plasmas as illustrated last year by publications [16–24]. Another motivation of this work is to study correlation effects in heavy systems. Er-like W^{6+} ion represent more interesting example as a Er-like Yb^{2+} that was investigated in Ref. [1]. In that paper was underlined that Yb ions represented an excellent example to study the correlation effects since they are very large, in part due to the $4f$ shell. The present case, Er-like W^{6+} ion, became even more complicated by the addition of the $5p$ shell (see Fig. 1), leading to the opportunity to study correlation effects between the $4f$ and $5p$ shells.

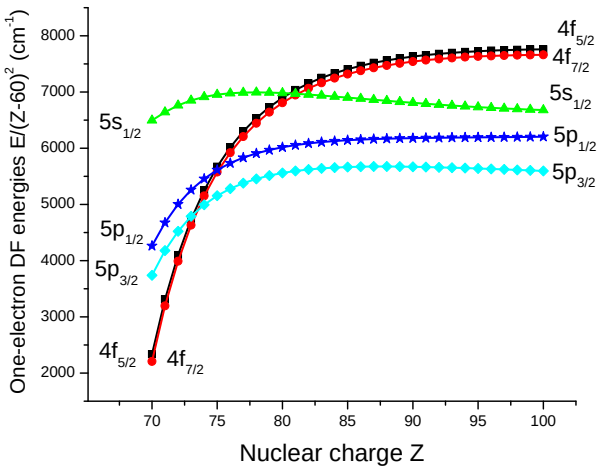

FIG. 1: Dirac-Fock (DF) binding energies of the $4f_j$, $5s_{1/2}$, and $5p_j$ orbitals as a function of Z.

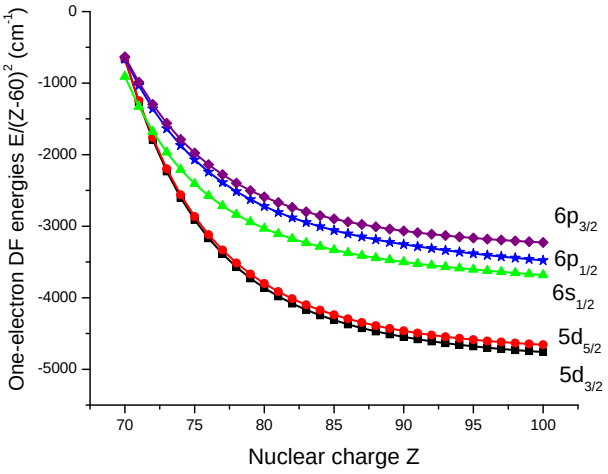

FIG. 2: Dirac-Fock (DF) valence energies of the $5d_j$, $6p_j$, $6s_{1/2}$ orbitals as a function of Z.

TABLE I: Possible hole-particle states in the $4f_j nl_{j'}(J) + 5p_j nl_{j'}(J)$ complexes; jj coupling schemes

Odd-parity states		Odd-parity states		Even-parity states		
$5p_{3/2}5d_{3/2}(0)$	$4f_{7/2}5d_{3/2}(2)$	$4f_{7/2}5d_{3/2}(3)$	$4f_{7/2}5d_{3/2}(4)$	$5p_{3/2}6p_{3/2}(0)$	$5p_{3/2}5f_{7/2}(2)$	$4f_{7/2}6p_{1/2}(4)$
$4f_{5/2}5d_{5/2}(0)$	$4f_{7/2}5d_{5/2}(2)$	$4f_{7/2}5d_{5/2}(3)$	$4f_{7/2}5d_{5/2}(4)$	$5p_{1/2}6p_{1/2}(0)$	$4f_{7/2}5f_{5/2}(2)$	$4f_{7/2}6p_{3/2}(4)$
$5p_{1/2}6s_{1/2}(0)$	$5p_{3/2}5d_{3/2}(2)$	$5p_{3/2}5d_{3/2}(3)$	$4f_{5/2}5d_{3/2}(4)$	$4f_{7/2}5f_{7/2}(0)$	$4f_{7/2}5f_{7/2}(2)$	$4f_{5/2}6p_{3/2}(4)$
$5p_{3/2}6d_{3/2}(0)$	$4f_{5/2}5d_{3/2}(2)$	$4f_{5/2}5d_{3/2}(3)$	$5p_{3/2}5d_{5/2}(4)$	$4f_{5/2}5f_{5/2}(0)$	$4f_{5/2}5f_{7/2}(2)$	$5p_{3/2}5f_{5/2}(4)$
$4f_{5/2}6d_{5/2}(0)$	$5p_{3/2}5d_{5/2}(2)$	$4f_{5/2}5d_{5/2}(3)$	$4f_{5/2}5d_{5/2}(4)$		$4f_{5/2}5f_{5/2}(2)$	$5p_{3/2}5f_{7/2}(4)$
$5p_{1/2}7s_{1/2}(0)$	$4f_{5/2}5d_{5/2}(2)$	$5p_{3/2}5d_{5/2}(3)$	$4f_{7/2}6s_{1/2}(4)$	$5p_{3/2}6p_{1/2}(1)$	$5p_{1/2}5f_{5/2}(2)$	$4f_{7/2}5f_{5/2}(4)$
	$5p_{1/2}5d_{3/2}(2)$	$5p_{1/2}5d_{5/2}(3)$	$4f_{7/2}6d_{3/2}(4)$	$5p_{3/2}6p_{3/2}(1)$		$4f_{7/2}5f_{7/2}(4)$
$5p_{3/2}5d_{3/2}(1)$	$5p_{3/2}6s_{1/2}(2)$	$4f_{7/2}6s_{1/2}(3)$	$4f_{7/2}6d_{5/2}(4)$	$4f_{5/2}6p_{3/2}(1)$	$5p_{3/2}6p_{3/2}(3)$	$4f_{5/2}5f_{5/2}(4)$
$4f_{7/2}5d_{5/2}(1)$	$4f_{5/2}6s_{1/2}(2)$	$4f_{5/2}6s_{1/2}(3)$	$5p_{3/2}6d_{5/2}(4)$	$5p_{1/2}6p_{1/2}(1)$	$4f_{7/2}6p_{1/2}(3)$	$4f_{5/2}5f_{7/2}(4)$
$4f_{5/2}5d_{5/2}(1)$	$5p_{1/2}5d_{5/2}(2)$	$4f_{7/2}6d_{3/2}(3)$	$4f_{5/2}6d_{3/2}(4)$	$5p_{1/2}6p_{3/2}(1)$	$4f_{5/2}6p_{1/2}(3)$	$5p_{1/2}5f_{7/2}(4)$
$4f_{5/2}5d_{3/2}(1)$	$4f_{7/2}6d_{3/2}(2)$	$4f_{7/2}6d_{5/2}(3)$	$4f_{5/2}6d_{5/2}(4)$	$5p_{3/2}5f_{5/2}(1)$	$4f_{7/2}6p_{3/2}(3)$	
$5p_{3/2}5d_{5/2}(1)$	$4f_{7/2}6d_{5/2}(2)$	$5p_{3/2}6d_{3/2}(3)$	$4f_{7/2}7s_{1/2}(4)$	$4f_{7/2}5f_{5/2}(1)$	$4f_{5/2}6p_{3/2}(3)$	$4f_{7/2}6p_{3/2}(5)$
$5p_{3/2}6s_{1/2}(1)$	$5p_{3/2}6d_{3/2}(2)$	$5p_{3/2}6d_{5/2}(3)$		$4f_{7/2}5f_{7/2}(1)$	$5p_{3/2}5f_{7/2}(3)$	$5p_{3/2}5f_{7/2}(5)$
$5p_{1/2}5d_{3/2}(1)$	$5p_{3/2}6d_{5/2}(2)$	$4f_{5/2}6d_{3/2}(3)$	$4f_{7/2}5d_{3/2}(5)$	$4f_{5/2}5f_{7/2}(1)$	$5p_{3/2}5f_{5/2}(3)$	$4f_{7/2}5f_{5/2}(5)$
$5p_{1/2}6s_{1/2}(1)$	$4f_{5/2}6d_{3/2}(2)$	$4f_{5/2}6d_{5/2}(3)$	$4f_{7/2}5d_{5/2}(5)$	$4f_{5/2}5f_{5/2}(1)$	$4f_{7/2}5f_{5/2}(3)$	$4f_{7/2}5f_{7/2}(5)$
$5p_{3/2}6d_{3/2}(1)$	$4f_{5/2}6d_{5/2}(2)$	$4f_{7/2}7s_{1/2}(3)$	$4f_{5/2}5d_{5/2}(5)$		$4f_{7/2}5f_{7/2}(3)$	$4f_{5/2}5f_{5/2}(5)$
$4f_{7/2}6d_{5/2}(1)$	$5p_{3/2}7s_{1/2}(2)$	$4f_{5/2}7s_{1/2}(3)$	$4f_{7/2}6d_{3/2}(5)$	$5p_{3/2}6p_{1/2}(2)$	$4f_{5/2}5f_{7/2}(3)$	$4f_{5/2}5f_{7/2}(5)$
$5p_{3/2}6d_{5/2}(1)$	$4f_{5/2}7s_{1/2}(2)$	$5p_{1/2}6d_{5/2}(3)$	$4f_{7/2}6d_{5/2}(5)$	$5p_{3/2}6p_{3/2}(2)$	$4f_{5/2}5f_{5/2}(3)$	
$4f_{5/2}6d_{5/2}(1)$	$5p_{1/2}6d_{3/2}(2)$		$4f_{5/2}6d_{5/2}(5)$	$4f_{5/2}6p_{1/2}(2)$	$5p_{1/2}5f_{5/2}(3)$	$4f_{7/2}5f_{5/2}(6)$
$4f_{5/2}6d_{3/2}(1)$	$5p_{1/2}6d_{5/2}(2)$			$4f_{7/2}6p_{3/2}(2)$	$5p_{1/2}5f_{7/2}(3)$	$4f_{7/2}5f_{7/2}(6)$
$5p_{3/2}7s_{1/2}(1)$			$4f_{7/2}5d_{5/2}(6)$	$4f_{5/2}6p_{3/2}(2)$		$4f_{5/2}5f_{7/2}(6)$
$5p_{1/2}6d_{3/2}(1)$			$4f_{7/2}6d_{5/2}(6)$	$5p_{1/2}6p_{3/2}(2)$		
$5p_{1/2}7s_{1/2}(1)$				$5p_{3/2}5f_{5/2}(2)$		$4f_{7/2}5f_{7/2}(7)$

II. METHOD

Details of the RMBPT method for hole-particle states were presented for calculation of energies in Ref. [31], for the calculation of multipole matrix elements for transitions from excited states into the ground state in Refs. [31–37], and for the calculation of multipole matrix elements for transitions between excited states in Refs. [38–40] . The calculations are carried out using a finite basis set of Dirac-Fock (DF) orbitals. These orbitals are obtained as linear combinations of B-splines determined using the method described in Ref. [41]. We use 50 B-splines of order 10 for each single-particle angular momentum state and include all orbitals with orbital angular momentum $l \leq 9$ in our basis set.

In addition to the $4f$ hole in the closed -shell [Cd]$4f^{14}5p^6$ ground state that was considered in Er-like Yb III [1], the $5p$ hole in the case of Er-like W VII should be considered (see Fig 1). The model space is formed from two hole-particle states of the type $a_v^+ a_a|0\rangle$ where $|0\rangle$ is the closed-shell [Cd]$4f_{5/2}^6 4f_{7/2}^8 5p_{1/2}^2 5p_{3/2}^4$ ground state, and a_i^+ and a_j are creation and annihilation operators, respectively. The single-particle indices v and a designate the valence and core states, respectively. For our study of low-lying states $4f^{-1}nl'$ and $5p^{-1}nl'$ states of Er-like ion, the values of a are $4f_{5/2}$, $4f_{7/2}$, $5p_{1/2}$, and $5p_{3/2}$ while the values of v are $6s_{1/2}$, $6p_{1/2}$, $6p_{3/2}$, $5d_{3/2}$, $5d_{5/2}$, $5f_{5/2}$, $5f_{7/2}$, $6d_{3/2}$, $6d_{5/2}$, and $7s_{1/2}$.

To obtain orthonormal model states, we consider the coupled states $\Phi_{JM}(av)$ defined by

$$\Phi_{JM}(av) = \sqrt{(2J+1)} \sum_{m_a m_v} (-1)^{j_v - m_v} \begin{pmatrix} j_v & J & j_a \\ -m_v & M & m_a \end{pmatrix} \times a^\dagger_{vm_v} a_{am_a} |0\rangle \,. \quad (1)$$

Combining the $4f_j$ and $5p_j$ hole orbitals and the $6s_{1/2}$, $6p_{1/2}$, $6p_{3/2}$, $5d_{3/2}$, $5d_{5/2}$, $5f_{5/2}$, $5f_{7/2}$, $6d_{3/2}$, $6d_{5/2}$, and $7s_{1/2}$ particle orbitals, the 80 odd-parity states are obtained consisting of 6 $J = 0$ states, 16 $J = 1$ states, 20 $J = 2$ states, 18 $J = 3$ states, 12 $J = 4$ states, six $J = 5$ states, and two $J = 6$ states. Additionally, there are 60 even-parity states consisting of 4 $J = 0$ states, 10 $J = 1$ states, 13 $J = 2$ states, 13 $J = 3$ states, 10 $J = 4$ states, six $J = 5$ states, three $J = 6$ states, and one $J = 7$ state. The distribution of the 140 states in the model space is summarized in Table I. Instead of using the $4f_j^{-1}nl'_{j'}$ and $5p_j^{-1}nl'_{j'}$ designations, we use simpler designations $4f_j nl'_{j'}$ and $5p_j nl'_{j'}$ in this table and in all following tables and the text below.

III. EXCITATION ENERGIES

In Table II, we give various contributions to the second-order energies for W VII ion. In this table, we show the one-body and two-body second-order Coulomb contributions to the energy matrix labeled $E_1^{(2)}$ and $E_2^{(2)}$, respectively. The corresponding Breit-Coulomb contributions are given in columns headed $B_1^{(2)}$ and $B_2^{(2)}$ of Table II. The one-body second-order energy is obtained

TABLE II: Second-order contributions to the energy matrices (a.u.) for odd-parity states with J=1 in the case of W VII. One-body and two-body second-order Coulomb and Breit-Coulomb contributions are given in columns labeled $E_1^{(2)}$, $E_2^{(2)}$, $B_1^{(2)}$, and $B_2^{(2)}$, respectively.

		Coulomb Interaction		Breit-Coulomb Correction	
$n_1l_1j_1\ n_2l_2j_2$	$n_3l_3j_3\ n_4l_4j_4$	$E_1^{(2)}$	$E_2^{(2)}$	$B_1^{(2)}$	$B_2^{(2)}$
$4f_{7/2}5d_{5/2}$	$4f_{7/2}5d_{5/2}$	-0.27870	0.15171	0.04163	0.00098
$4f_{5/2}5d_{5/2}$	$4f_{5/2}5d_{5/2}$	-0.29003	0.10659	0.04240	0.00109
$4f_{5/2}5d_{3/2}$	$4f_{5/2}5d_{3/2}$	-0.29625	0.13188	0.04198	0.00132
$4f_{7/2}6d_{5/2}$	$4f_{7/2}6d_{5/2}$	-0.22777	0.01117	0.04691	0.00026
$4f_{5/2}6d_{5/2}$	$4f_{5/2}6d_{5/2}$	-0.23910	0.00959	0.04768	0.00026
$4f_{5/2}6d_{3/2}$	$4f_{5/2}6d_{3/2}$	-0.23995	0.01119	0.04764	0.00033
$4f_{7/2}5d_{5/2}$	$4f_{5/2}5d_{5/2}$	0.00000	-0.00328	0.00000	0.00000
$4f_{5/2}5d_{5/2}$	$4f_{7/2}5d_{5/2}$	0.00000	-0.00957	0.00000	-0.00001
$4f_{7/2}5d_{5/2}$	$4f_{5/2}6d_{5/2}$	0.00000	-0.00480	0.00000	-0.00014
$4f_{5/2}6d_{5/2}$	$4f_{7/2}5d_{5/2}$	0.00000	0.00601	0.00000	0.00011
$5p_{3/2}5d_{3/2}$	$5p_{3/2}5d_{3/2}$	-0.03151	0.01337	0.00449	0.00098
$5p_{3/2}5d_{5/2}$	$5p_{3/2}5d_{5/2}$	-0.02529	-0.14426	0.00490	0.00060
$5p_{1/2}5d_{3/2}$	$5p_{1/2}5d_{3/2}$	-0.04137	0.02475	0.00606	0.00086
$5p_{3/2}6d_{3/2}$	$5p_{3/2}6d_{3/2}$	0.02479	-0.00803	0.01015	0.00030
$5p_{3/2}6d_{5/2}$	$5p_{3/2}6d_{5/2}$	0.02564	-0.00921	0.01018	0.00025
$5p_{1/2}6d_{3/2}$	$5p_{1/2}6d_{3/2}$	0.01492	-0.01655	0.01172	0.00032
$5p_{3/2}6s_{1/2}$	$5p_{3/2}6s_{1/2}$	0.03736	-0.08485	0.00893	0.00054
$5p_{1/2}6s_{1/2}$	$5p_{1/2}6s_{1/2}$	0.02750	-0.08996	0.01050	0.00061
$5p_{3/2}7s_{1/2}$	$5p_{3/2}7s_{1/2}$	0.02965	-0.00403	0.01063	0.00025
$5p_{1/2}7s_{1/2}$	$5p_{1/2}7s_{1/2}$	0.01979	-0.00534	0.01220	0.00026
$5p_{3/2}5d_{3/2}$	$5p_{1/2}5d_{3/2}$	0.00000	-0.03682	0.00000	-0.00009
$5p_{1/2}5d_{3/2}$	$5p_{3/2}5d_{3/2}$	0.00000	-0.00441	0.00000	-0.00008
$5p_{3/2}5d_{3/2}$	$5p_{3/2}6d_{3/2}$	0.00000	0.02135	0.00000	-0.00034
$5p_{3/2}6d_{3/2}$	$5p_{3/2}5d_{3/2}$	0.00000	-0.05294	0.00000	-0.00028

as a sum of the valence $E_v^{(2)}$ and hole $E_a^{(2)}$ energies with the later being the dominant contribution.

The values of $E_1^{(2)}$ and $B_1^{(2)}$ are non-zero only for diagonal matrix elements. There are 140 diagonal and more than 10000 non-diagonal matrix elements for the $4f_jnl_{j'}\,(J)$ and $5p_jnl_{j'}\,(J)$ hole-particle states, and for illustration only the part of odd-parity subset with J=1 is shown in Table II. The second-order Breit-Coulomb corrections are relatively large and, therefore, must be included in accurate calculations. The values of non-diagonal matrix elements given in columns headed $E_2^{(2)}$ and $B_2^{(2)}$ are comparable with values of diagonal two-body matrix elements. However, the values of one-body contributions, $E_1^{(2)}$ and $B_1^{(2)}$, are larger than the values of two-body contributions, $E_2^{(2)}$ and $B_2^{(2)}$ in the case of the $4f_jnl_{j'}\,(1)$ matrix elements. In the case of the $5p_jnl_{j'}\,(1)$ matrix elements, the values of one-body contributions, $E_1^{(2)}$, are comparable with the values of two-body contributions, $E_2^{(2)}$, and they cancel each other for some matrix elements. One can see from Table II that the one-body contributions $E_1^{(2)}$ and $B_1^{(2)}$ for the $4f_jnl_{j'}\,(1)$ matrix elements are larger than for the $5p_jnl_{j'}\,(1)$ matrix elements. The same ratios (about 10) was found for the diagonal two-body $4f_jnl_{j'}\,(1)$ and $5p_jnl_{j'}\,(1)$ matrix elements.

In Table III, we present results for the zeroth-, first-, and second-order Coulomb contributions, $E^{(0)}$, $E^{(1)}$, and $E^{(2)}$, and the first- and second-order Breit-Coulomb corrections, $B^{(1)}$ and $B^{(2)}$. Importance of correlation contribution is evident from this table; the ratio of the first and zeroth orders ($E^{(1)}/E^{(0)}$) is about 10–30%, and the ratio of the second and first ($E^{(2)}/E^{(1)}$) orders is even larger, 20–60% for the $4f_jnl_{j'}\,(1)$ matrix elements, while $E^{(2)}/E^{(1)}$ ratio for the $5p_jnl_{j'}\,(1)$ matrix elements is about 3–5 % only. The $E^{(1)}$ and $E^{(2)}$ contributions for the $5p_jnl_{j'}\,(1)$ and $4f_jnl_{j'}\,(1)$ non-diagonal matrix elements differ by a factor of 5–10. The values of the $5p_jnl_{j'}\,(1)$ diagonal and non-diagonal matrix elements are comparable for the $E^{(1)}$ and $E^{(2)}$ contributions while the ratio of the $4p_jnl_{j'}\,(1)$ diagonal and non-diagonal matrix elements ranges from 10 to 50. The corrections for the frequency-dependent Breit interaction [42] are included to the first order only. The difference between the first-order Breit corrections calculated with and without frequency dependence is 1–3%, however, the ratio of the first-order Breit and Coulomb corrections is also 2–5%. As illustrated in Table III, the first-order non-diagonal matrix elements are symmetric, but the second-order non-diagonal matrix elements are nonsymmetrical. The values of the $E^{(2)}[a'v'(J), av(J)]$ and $E^{(2)}[av(J), a'v'(J)]$ matrix elements differ in some cases by a factor 2–3 and occasionally have opposite signs.

TABLE III: Contributions to the energy matrix $E[n_1 j_1\ nl_2 j_2, n_3 j_3\ nl_4 j_4] = E^{(0)} + E^{(1)} + E^{(2)} + B^{(1)} + B^{(2)}$ before diagonalization. These contributions are given for W VII ion with a [Cd]$4f^{14}5p^6$ core, in the case of odd-parity states with J=1.

$n_1 l_1 j_1\ n_2 l_2 j_2$	$n_3 l_3 j_3\ n_4 l_4 j_4$	$E^{(0)}$	$E^{(1)}$	$B^{(1)}$	$E^{(2)}$	$B^{(2)}$
$4f_{7/2}5d_{5/2}$	$4f_{7/2}5d_{5/2}$	2.31343	-0.67451	-0.00987	-0.12699	0.04261
$4f_{5/2}5d_{5/2}$	$4f_{5/2}5d_{5/2}$	2.40214	-0.72688	-0.01364	-0.18345	0.04348
$4f_{5/2}5d_{3/2}$	$4f_{5/2}5d_{3/2}$	2.36577	-0.69657	-0.01268	-0.16437	0.04330
$4f_{7/2}6d_{5/2}$	$4f_{7/2}6d_{5/2}$	3.44592	-0.34349	-0.01211	-0.21660	0.04717
$4f_{5/2}6d_{5/2}$	$4f_{5/2}6d_{5/2}$	3.53462	-0.35362	-0.01589	-0.22952	0.04794
$4f_{5/2}6d_{3/2}$	$4f_{5/2}6d_{3/2}$	3.52265	-0.34878	-0.01567	-0.22876	0.04797
$4f_{7/2}5d_{5/2}$	$4f_{5/2}5d_{5/2}$	0.00000	-0.02776	0.00000	-0.00328	0.00000
$4f_{5/2}5d_{5/2}$	$4f_{7/2}5d_{5/2}$	0.00000	-0.02776	0.00000	-0.00957	-0.00001
$4f_{7/2}5d_{5/2}$	$4f_{5/2}6d_{5/2}$	0.00000	0.01184	0.00000	-0.00480	-0.00014
$4f_{5/2}6d_{5/2}$	$4f_{7/2}5d_{5/2}$	0.00000	0.01184	0.00000	0.00601	0.00011
$5p_{3/2}5d_{3/2}$	$5p_{3/2}5d_{3/2}$	2.13678	-0.61095	-0.00479	-0.01813	0.00547
$5p_{3/2}5d_{5/2}$	$5p_{3/2}5d_{5/2}$	2.17314	-0.37203	-0.00578	-0.16955	0.00549
$5p_{1/2}5d_{3/2}$	$5p_{1/2}5d_{3/2}$	2.55005	-0.48271	-0.01020	-0.01662	0.00692
$5p_{3/2}6d_{3/2}$	$5p_{3/2}6d_{3/2}$	3.29366	-0.33097	-0.00771	0.01676	0.01045
$5p_{3/2}6d_{5/2}$	$5p_{3/2}6d_{5/2}$	3.30563	-0.30359	-0.00793	0.01643	0.01043
$5p_{1/2}6d_{3/2}$	$5p_{1/2}6d_{3/2}$	3.70693	-0.31259	-0.01308	-0.00162	0.01204
$5p_{3/2}6s_{1/2}$	$5p_{3/2}6s_{1/2}$	2.48895	-0.43706	-0.00642	-0.04749	0.00948
$5p_{1/2}6s_{1/2}$	$5p_{1/2}6s_{1/2}$	2.90222	-0.45246	-0.01178	-0.06246	0.01111
$5p_{3/2}7s_{1/2}$	$5p_{3/2}7s_{1/2}$	3.36777	-0.27475	-0.00779	0.02562	0.01088
$5p_{1/2}7s_{1/2}$	$5p_{1/2}7s_{1/2}$	3.78104	-0.27957	-0.01315	0.01445	0.01246
$5p_{3/2}5d_{3/2}$	$5p_{1/2}5d_{3/2}$	0.00000	-0.12848	-0.00003	-0.05000	-0.00017
$5p_{1/2}5d_{3/2}$	$5p_{3/2}5d_{3/2}$	0.00000	-0.12848	-0.00003	-0.05469	-0.00017
$5p_{3/2}5d_{3/2}$	$5p_{3/2}6d_{3/2}$	0.00000	0.09060	0.00000	0.02135	-0.00034
$5p_{3/2}6d_{3/2}$	$5p_{3/2}5d_{3/2}$	0.00000	0.09060	0.00000	-0.05294	-0.00028

TABLE IV: Energies of W VII for odd-parity states with J=1 relative to the ground state. $E^{(0+1)} \equiv E^{(0)} + E^{(1)} + B^{(1)}$

jj coupl.	$E^{(0+1)}$	$E^{(2)}$	$B^{(2)}$	$E_{\rm LS}$	$E_{\rm tot}$
$4f_{7/2}5d_{5/2}$	344240	-33353	9453	26	320366
$4f_{5/2}5d_{5/2}$	363026	-38703	9561	175	334058
$4f_{5/2}5d_{3/2}$	370740	-25476	9450	37	354750
$4f_{7/2}6d_{5/2}$	680361	-49855	10335	114	640955
$4f_{5/2}6d_{5/2}$	695630	-52293	10505	-114	653728
$4f_{5/2}6d_{3/2}$	697840	-52647	10498	-114	655576
$5p_{3/2}5d_{3/2}$	319465	-15808	1201	-908	303950
$5p_{3/2}5d_{5/2}$	380722	-5907	1360	-736	375439
$5p_{1/2}5d_{3/2}$	447602	-12102	2089	877	438465
$5p_{3/2}6d_{3/2}$	475215	-21611	1400	-553	454451
$5p_{3/2}6d_{5/2}$	533681	-15281	2450	413	521263
$5p_{1/2}6d_{3/2}$	648575	3433	2279	872	655159
$5p_{3/2}6s_{1/2}$	659770	2889	2281	873	665813
$5p_{1/2}6s_{1/2}$	678408	6955	2378	882	688623
$5p_{3/2}7s_{1/2}$	743278	-570	2628	412	745748
$5p_{1/2}7s_{1/2}$	767143	4754	2724	413	775034

We now discuss how the final energy levels are obtained from the above contributions. To determine the first-order energies of the states under consideration, we diagonalize the symmetric first-order effective Hamiltonian, including both Coulomb and Breit interactions. The first-order expansion coefficient $C^N[av(J)]$ (often called a mixing coefficient) is the N-th eigenvector of the first-order effective Hamiltonian, and $E^{(1)}[N]$ is the corresponding eigenvalue. The resulting eigenvectors are used to determine the second-order Coulomb correction $E^{(2)}[N]$, the second-order Breit-Coulomb correction $B^{(2)}[N]$ and the QED correction $E_{\rm LS}[N]$.

In Table IV, the following contributions to the energies of 16 excited states in W^{6+} are listed: the sum of the zeroth and first-order energies $E^{(0+1)} = E^{(0)} + E^{(1)} + B^{(1)}$, the second-order Coulomb energy $E^{(2)}$, the second-order Breit-Coulomb correction $B^{(2)}$, the QED correction $E_{\rm LS}$, and the sum of the above contributions $E_{\rm tot}$. The Lamb shift $E_{\rm LS}$ is approximated as the sum of the one-electron self energy and the first-order vacuum-polarization energy. The vacuum-polarization contribution is calculated from the Uehling potential using the results of Fullerton and Rinker [43]. The self-energy contribution is estimated for the $s_{1/2}$, $p_{1/2}$ and $p_{3/2}$ orbitals by interpolating among the values obtained by Mohr [44, 45, 46] using Coulomb wave functions. For this purpose, an effective nuclear charge $Z_{\rm eff}$ is obtained by finding the value of $Z_{\rm eff}$ required to give a Coulomb orbital with the same average $\langle r \rangle$ as the DHF orbital.

When starting calculations from relativistic DF wave functions, it is natural to use jj designations for uncoupled energy matrix elements; however, neither jj nor LS coupling describes the *physical* states properly. We find out that the mixing coefficients are equal to 0.5–0.7 in the

TABLE V: Energies (10^3cm^{-1}) of odd- and even-parity states relative to the ground state in W VII calculated in the first-order and second-order RMBPTI and RMBPT values are compared with recommended NIST data [15].

Level	RMBPT1	RMBPT	NIST	Level	RMBPT1	RMBPT	NIST	Level	RMBPT1	RMBPT	NIST
$4f_{7/2}5d_{3/2}(2)$	329.329	304.356	311.441	$5p_{3/2}6p_{1/2}(2)$	521.041	524.176	534.428	$4f_{7/2}6d_{5/2}(6)$	679.338	639.405	648.072
$5p_{3/2}5d_{3/2}(0)$	312.772	315.228	315.259	$4f_{7/2}6p_{3/2}(3)$	565.479	525.104	534.838	$4f_{5/2}5f_{7/2}(5)$	688.657	639.461	647.862
$4f_{7/2}5d_{3/2}(5)$	335.243	309.795	318.185	$4f_{7/2}6p_{3/2}(4)$	566.340	526.136	536.420	$4f_{7/2}6d_{5/2}(2)$	679.646	639.802	648.558
$5p_{3/2}5d_{3/2}(1)$	319.465	303.950	318.899	$4f_{5/2}6p_{3/2}(1)$	581.089	538.219	538.903	$5p_{3/2}5f_{7/2}(5)$	640.731	640.193	
$4f_{7/2}5d_{3/2}(3)$	339.612	314.129	320.693	$4f_{5/2}6p_{3/2}(4)$	582.739	540.187	551.684	$4f_{7/2}6d_{5/2}(1)$	680.361	640.834	649.982
$4f_{7/2}5d_{3/2}(4)$	341.947	315.942	322.527	$4f_{5/2}6p_{3/2}(2)$	583.801	541.150	543.641	$4f_{7/2}6d_{5/2}(4)$	680.687	640.880	649.401
$4f_{7/2}5d_{5/2}(6)$	344.131	318.698	327.044	$4f_{5/2}6p_{3/2}(3)$	584.739	542.073	539.129	$4f_{7/2}6d_{5/2}(3)$	680.620	640.944	649.662
$4f_{7/2}5d_{5/2}(1)$	344.240	320.218	330.825	$5p_{3/2}6p_{3/2}(3)$	539.002	542.525	553.588	$4f_{7/2}6d_{5/2}(5)$	680.900	641.174	650.367
$4f_{7/2}5d_{5/2}(2)$	346.650	321.161	328.020	$5p_{3/2}6p_{3/2}(1)$	539.954	544.143	549.865	$5p_{3/2}5f_{5/2}(4)$	641.479	641.444	
$4f_{7/2}5d_{5/2}(4)$	350.706	325.059	329.950	$5p_{3/2}6p_{3/2}(2)$	544.222	548.951	552.671	$5p_{3/2}5f_{7/2}(4)$	645.911	644.724	
$4f_{7/2}5d_{5/2}(3)$	351.835	326.304	333.095	$5p_{3/2}6p_{3/2}(0)$	552.987	552.510	550.082	$4f_{5/2}5f_{5/2}(0)$	714.711	647.558	
$4f_{7/2}5d_{5/2}(5)$	353.142	327.172	335.017	$5p_{1/2}6p_{1/2}(1)$	608.399	608.918		$5p_{3/2}5f_{7/2}(2)$	646.962	649.371	
$4f_{5/2}5d_{3/2}(4)$	354.217	327.296	335.411	$5p_{1/2}6p_{1/2}(0)$	619.025	613.601		$4f_{5/2}6d_{3/2}(4)$	694.761	652.252	662.413
$4f_{5/2}5d_{3/2}(2)$	356.714	328.052	337.854	$4f_{7/2}5f_{5/2}(1)$	665.755	618.305		$5p_{3/2}6d_{3/2}(0)$	646.752	652.544	
$4f_{5/2}5d_{5/2}(0)$	355.685	329.046	339.629	$4f_{7/2}5f_{7/2}(1)$	667.382	619.607	626.581	$4f_{5/2}6d_{3/2}(2)$	695.353	652.859	
$5p_{3/2}5d_{3/2}(2)$	331.623	332.615	335.017	$4f_{7/2}5f_{5/2}(6)$	667.639	620.167	626.291	$4f_{5/2}6d_{5/2}(1)$	695.630	653.634	665.763
$5p_{3/2}5d_{3/2}(3)$	331.581	333.345	335.171	$4f_{7/2}5f_{5/2}(2)$	667.416	620.366	626.025	$4f_{5/2}6d_{3/2}(3)$	696.272	653.973	664.543
$4f_{5/2}5d_{5/2}(1)$	363.026	333.965	339.705	$4f_{7/2}5f_{7/2}(7)$	667.746	620.719	627.487	$4f_{5/2}6d_{5/2}(0)$	696.833	654.283	
$4f_{5/2}5d_{3/2}(3)$	362.318	334.616	343.093	$4f_{7/2}5f_{5/2}(3)$	668.406	621.450	627.063	$5p_{3/2}6d_{3/2}(1)$	648.575	655.159	647.462
$5p_{3/2}5d_{5/2}(4)$	333.091	335.123	340.530	$4f_{7/2}5f_{7/2}(3)$	669.393	622.274	629.102	$4f_{5/2}6d_{3/2}(1)$	697.840	655.490	665.445
$4f_{5/2}5d_{5/2}(5)$	364.731	337.637	346.385	$4f_{7/2}5f_{5/2}(5)$	669.604	622.381	628.672	$4f_{5/2}6d_{5/2}(5)$	698.225	655.897	666.177
$4f_{5/2}5d_{5/2}(2)$	366.972	339.224	348.370	$4f_{7/2}5f_{5/2}(4)$	669.425	622.425	628.049	$5p_{3/2}6d_{3/2}(3)$	649.958	656.305	650.474
$5p_{3/2}5d_{5/2}(2)$	340.366	342.283	343.305	$4f_{7/2}5f_{7/2}(2)$	669.537	622.553	629.962	$4f_{5/2}6d_{5/2}(2)$	698.640	656.353	663.215
$4f_{5/2}5d_{5/2}(3)$	370.524	342.542	351.600	$4f_{7/2}5f_{7/2}(0)$	675.576	622.838		$4f_{5/2}6d_{5/2}(3)$	699.283	657.037	667.394
$4f_{5/2}5d_{5/2}(4)$	371.765	344.093	352.478	$4f_{7/2}5f_{7/2}(6)$	669.957	623.242	630.282	$4f_{5/2}6d_{5/2}(4)$	699.504	657.285	
$5p_{3/2}5d_{5/2}(3)$	351.853	354.188	354.111	$4f_{7/2}5f_{7/2}(5)$	669.918	623.258	630.395	$5p_{3/2}6d_{3/2}(2)$	651.377	657.649	653.950
$4f_{5/2}5d_{3/2}(1)$	370.740	354.690	345.394	$4f_{7/2}5f_{7/2}(4)$	670.086	623.282	629.791	$5p_{3/2}6d_{5/2}(4)$	652.242	658.663	652.662
$5p_{3/2}5d_{5/2}(1)$	380.722	375.439	382.577	$5p_{3/2}5f_{5/2}(2)$	641.062	626.909	632.406	$5p_{3/2}6d_{5/2}(2)$	653.787	660.333	
$4f_{7/2}6s_{1/2}(4)$	464.328	406.832	437.188	$5p_{1/2}6p_{3/2}(2)$	628.773	627.938		$5p_{3/2}6d_{5/2}(3)$	655.651	662.526	656.165
$4f_{7/2}6s_{1/2}(3)$	465.092	407.757	438.026	$5p_{1/2}6p_{3/2}(1)$	629.229	630.971		$5p_{3/2}6d_{5/2}(1)$	659.770	665.813	658.367
$5p_{1/2}5d_{3/2}(2)$	414.843	418.044		$5p_{3/2}5f_{7/2}(3)$	643.218	635.058		$4f_{7/2}7s_{1/2}(4)$	705.126	669.277	675.864
$4f_{5/2}6s_{1/2}(2)$	482.856	422.904	454.566	$4f_{5/2}5f_{7/2}(1)$	684.883	635.173	642.481	$4f_{7/2}7s_{1/2}(3)$	705.307	669.425	676.159
$4f_{5/2}6s_{1/2}(3)$	483.451	423.609	455.221	$4f_{7/2}6d_{3/2}(2)$	675.442	635.370		$4f_{5/2}7s_{1/2}(2)$	723.736	685.426	693.250
$5p_{3/2}6s_{1/2}(2)$	443.640	429.403	443.237	$4f_{5/2}5f_{5/2}(1)$	686.186	636.005	643.880	$4f_{5/2}7s_{1/2}(3)$	723.868	685.545	693.468
$5p_{1/2}5d_{5/2}(2)$	425.582	430.763		$4f_{7/2}6d_{3/2}(5)$	676.242	636.260	645.238	$5p_{3/2}7s_{1/2}(2)$	677.480	687.212	678.949
$5p_{1/2}5d_{5/2}(3)$	430.896	434.054		$4f_{5/2}5f_{5/2}(5)$	686.225	636.269	643.569	$5p_{3/2}7s_{1/2}(1)$	678.408	688.623	680.153
$5p_{3/2}6s_{1/2}(1)$	447.602	438.465	446.749	$4f_{7/2}6d_{3/2}(3)$	677.008	637.107	645.943	$5p_{1/2}5f_{5/2}(2)$	733.376	690.387	
$5p_{1/2}5d_{3/2}(1)$	475.215	454.451	462.496	$4f_{5/2}5f_{7/2}(6)$	686.715	637.289	645.507	$5p_{1/2}5f_{5/2}(3)$	731.174	733.382	
$4f_{7/2}6p_{1/2}(3)$	543.683	503.159	512.882	$4f_{5/2}5f_{7/2}(2)$	686.869	637.487	646.444	$5p_{1/2}5f_{7/2}(4)$	732.151	737.062	
$4f_{7/2}6p_{1/2}(4)$	544.148	503.412	513.640	$4f_{7/2}6d_{3/2}(4)$	677.480	637.579	646.596	$5p_{1/2}6d_{3/2}(2)$	738.932	742.200	
$5p_{1/2}6s_{1/2}(0)$	531.577	518.773		$5p_{3/2}5f_{5/2}(3)$	645.211	637.769		$5p_{1/2}6d_{5/2}(2)$	742.363	745.216	
$4f_{5/2}6p_{1/2}(3)$	562.227	519.298	530.489	$4f_{5/2}5f_{7/2}(3)$	687.635	638.093	643.867	$5p_{1/2}6d_{3/2}(1)$	743.278	745.748	740.964
$4f_{5/2}6p_{1/2}(2)$	563.041	521.117	519.194	$5p_{3/2}5f_{5/2}(1)$	638.843	638.336		$5p_{1/2}6d_{5/2}(3)$	742.920	746.427	
$5p_{1/2}6s_{1/2}(1)$	533.681	521.263	531.465	$4f_{5/2}5f_{5/2}(2)$	687.938	638.395	645.907	$5p_{1/2}5f_{7/2}(3)$	731.741	758.593	
$5p_{3/2}6p_{1/2}(1)$	518.746	522.071	517.074	$4f_{5/2}5f_{5/2}(3)$	688.130	638.537	646.673	$5p_{1/2}7s_{1/2}(0)$	766.706	774.403	
$4f_{7/2}6p_{3/2}(2)$	564.063	522.898	531.434	$4f_{5/2}5f_{5/2}(4)$	688.422	638.779	646.733	$5p_{1/2}7s_{1/2}(1)$	767.143	775.034	766.776
$4f_{7/2}6p_{3/2}(5)$	563.659	523.453	533.693	$4f_{5/2}5f_{7/2}(4)$	688.542	639.323	647.578				

cases considered in this work. Therefore, we still use the jj designations in Table IV. We already mentioned the importance of including the correlation contribution in order to obtain accurate energy values for Er-like W VII ion. The second-order Coulomb contribution $E^{(2)}$ gives 10% to the total values of the $4f_j5d_{j'}$ (1) and $4f_j6d_{j'}$ (1) energies. The second-order Coulomb contribution $E^{(2)}$ for the $5p_{j'}nl_j$ (1) energies is much smaller (1–4 %). The $E^{(2)}$ values are very different for the $5p_{j'}nl_j$ (1) levels; ranging from the negative -21611 cm^{-1} up to the positive 6955 cm^{-1} value. Such a large difference in the second-order contribution is due to large values of non-diagonal matrix elements illustrated by Table III.

In Table V, we compare our RMBPT results for the $4f5d$, $4f6d$, $4f6s$, $4f7s$, $4f6p$, $4f5f$, $5p5d$, $5d6d$, $5s6s$, $5s7s$, $5p6p$, and $5p5f$ excitation energies in W VII with recommended NIST data [15]. The difference between

TABLE VI: Wavelengths (λ in Å) for the dipole transitions calculated by RMBPT, COWAN, and HULLAC codes are compared with recommended NIST data [15].

Level	NIST	RMBPT1	RMBPT	COWAN	HULLAC
$5p_{1/2}7s_{1/2}(1)$	130.416	130.354	129.027	131.621	125.496
$5p_{1/2}6d_{3/2}(1)$	134.959	134.539	134.094	136.060	127.003
$5p_{3/2}7s_{1/2}(1)$	147.026	147.404	145.217	146.836	139.624
$4f_{5/2}6d_{5/2}(1)$	150.204	143.755	152.991	151.008	140.003
$4f_{5/2}6d_{3/2}(1)$	150.275	143.299	152.558	153.233	145.055
$5p_{3/2}6d_{5/2}(1)$	151.891	151.568	150.192	153.602	151.394
$4f_{7/2}6d_{5/2}(1)$	153.850	146.981	156.047	153.945	151.526
$5p_{3/2}6d_{3/2}(1)$	154.449	154.184	152.635	156.752	154.789
$5p_{1/2}6s_{1/2}(1)$	188.159	187.378	191.842	189.716	175.145
$5p_{1/2}5d_{3/2}(1)$	216.218	210.431	220.046	218.516	189.482
$5p_{3/2}6s_{1/2}(1)$	223.839	223.413	228.068	222.230	203.377
$5p_{3/2}5d_{5/2}(1)$	261.385	262.659	266.355	263.682	227.824
$4f_{5/2}5d_{3/2}(1)$	289.525	269.731	281.937	301.280	263.649
$4f_{5/2}5d_{5/2}(1)$	294.373	275.462	299.433	304.528	286.599
$4f_{7/2}5d_{5/2}(1)$	302.275	290.495	312.287	306.277	289.190
$5p_{3/2}5d_{3/2}(1)$	313.579	313.023	329.001	319.170	305.513

our RMBPT values and NIST data is about 1–2 % for the most of cases except for the $5p_{3/2}5d_{3/2}(1)$ and $4f_j6s_{1/2}(J)$ levels where the difference is about 6 %. This large difference is likely due to large contributions of the correlation effects.

To demonstrate the size of the correlation contribution, we added the data evaluated in the first-order approximation in Table V (see the column labelled 'RMBPT1'). These data are obtained as a sum of the $E^{(0)}$, $E^{(1)}$, and $B^{(1)}$ values (see explanation of Table IV). These 'RMBPT1' values are often referred to as the MCDF values [47]. The difference between the values in the 'RMBPT1' and 'RMBPT' columns range from 1 % to 5% except for the $4f_j6s_{1/2}(J)$ levels where the difference is about 14 %. The difference between the RMBPT1 and RMBPT values is about 5 % for the $5p_{3/2}5d_{3/2}(1)$ level. For this level, the RMBPT1 value is in excellent agreement with the NIST value (only 0.2 % difference). We would like to mention that our RMBPT results presented in Table V are first *ab initio* values for the energy levels in W VII ion.

To ensure that the accuracy of our results obtained by RMBPT code is good in comparison with results obtained by other frequently used codes, we evaluate energies and wavelengths in W VII ion using the HULLAC and COWAN codes also. In Table VI, we list wavelengths for the 16 dipole transitions calculated using these codes. The scaling of electrostatic integrals in the COWAN code provides a possibility to correct the correlation effects and to obtain a good agreement with experimental energies. In the HULLAC code, the intermediate-coupling energies are calculated using the relativistic version of the parametric potential method, including configuration mixing. Example of such calculations are given in Table VI. We find the smallest difference between values given in the column 'NIST' and the columns 'RMBPT' and 'COWAN'. There are only three cases among 16 cases when the difference is larger than 2 %. The largest disagreement with NIST values is found for values obtained by HULLAC code. Such comparison is very useful to check the accuracy of different codes. It is specially useful for predictions such as done previously by us in Refs. [10–12].

IV. MULTIPOLE TRANSITIONS FROM EXCITED STATES INTO THE GROUND STATE

The first 140 excited states in Er-like W ions are the [Cd]$4f^{13}5p^6nl$ and [Cd]$4f^{14}5p^5nl$ states. There are 124 metastable levels with $J = 0$, 2 - 5, but only 16 levels with dipole transitions ($J = 1$) to the ground state. Below, we consider all possible multipole (E1, E2, E3, M1, M2, and M3) transitions from the [Cd]$4f^{13}5p^6nl$ and [Cd]$4f^{14}5p^5nl$ states to the [Cd]$4f^{14}5p^6$ ground state in Er-like W^{6+} ions.

We calculate electric-dipole (E1) matrix elements for the transitions between the sixteen odd-parity $4f_j5d_{j'}(1)$, $4f_j6d_{j'}(1)$, $5p_j5d_{j'}(1)$, $5p_j6d_{j'}(1)$, $5p_j6s_{1/2}(1)$, and $5p_j7s_{1/2}(1)$ excited states and the ground state, magnetic-quadrupole (M2) matrix elements between the 20 odd-parity $4f_j5d_{j'}(2)$, $4f_j6d_{j'}(2)$, $4f_j6s_{1/2}(2)$, $4f_j7s_{1/2}(2)$, $5p_j5d_{j'}(2)$, $5p_j6d_{j'}(2)$, $5p_j6s_{1/2}(2)$, and $5p_j7s_{1/2}(2)$ excited states and the ground state, and electric-octupole (E3) matrix elements between the 18 odd-parity $4f_j5d_{j'}(3)$, $4f_j6d_{j'}(3)$, $4f_j6s_{1/2}(3)$, $4f_j7s_{1/2}(3)$, $5p_j5d_{j'}(3)$, and $5p_j6d_{j'}(3)$ excited states and the ground state.

Magnetic-dipole (M1) matrix elements for the transitions between the ten even-parity $4f_j5f_{j'}(1)$, $4f_j6p_{j'}(1)$, $5p_j5f_{j'}(1)$, and $5p_j6p_{j'}(1)$, excited states and the ground state, electric-quadrupole (E2) matrix elements between the 13 even-parity $4f_j5f_{j'}(2)$, $4f_j6p_{j'}(2)$, $5p_j5f_{j'}(2)$, and $5p_j6p_{j'}(2)$ excited states and the ground state, and magnetic-octupole (M3) matrix elements between the 13 even-parity $4f_j5f_{j'}(3)$, $4f_j6p_{j'}(3)$, $5p_j5f_{j'}(3)$, and $5p_j6p_{j'}(3)$ excited states and the ground state are computed.

Analytical expressions for the first and the second order RMBPT are given by Eqs. (2.12)-(2.17) of Ref. [31] for the E1 matrix elements and in Refs. [33, 35, 36] for the M1, M2, M3, E2, and E3 matrix elements.

We refer the first- and second-order Coulomb corrections and second-order Breit-Coulomb corrections to reduced multipole matrix elements as $Z^{(1)}$, $Z^{(2)}$, and $B^{(2)}$, respectively, throughout the text. In Table VII, we list values of *uncoupled* first- and second-order E1, E2, E3, M1, M2, and M3 matrix elements $Z^{(1)}$, $Z^{(2)}$, $B^{(2)}$, together with derivative terms $P^{(\mathrm{derv})}$, for Er-like W^{6+} (see, for detail, Refs. [1, 33, 35, 36]).

Importance of correlation contributions is evident from this table; the ratio of the second and first ($Z^{(2)}/Z^{(1)}$) orders is about 10-30% for most of the E1 transitions, except for the $5p_{3/2}6d_j(1)$ and $5p_{1/2}7s_{1/2}(1)$ states when

TABLE VII: E1, E2, E3, M1, M2, and M3 uncoupled reduced matrix elements in length form for transitions from $av(J)$ states with J=1, 2, and 3 into the ground state in W VII.

$av(J)$	$Z^{(1)}$	$Z^{(2)}$	$B^{(2)}$	$P^{(\mathrm{derv})}$	$av(J)$	$Z^{(1)}$	$Z^{(2)}$	$B^{(2)}$	$P^{(\mathrm{derv})}$
E1 uncoupled reduced matrix elements					M1 uncoupled reduced matrix elements				
$4f_{7/2}5d_{5/2}(1)$	-0.6510	0.1093	-0.0013	-0.6510	$4f_{5/2}6p_{3/2}(1)$	0.0000	-0.0025	0.0000	0.0000
$4f_{5/2}5d_{3/2}(1)$	-0.5426	0.1001	-0.0013	-0.5426	$4f_{7/2}5f_{5/2}(1)$	-0.0102	-0.0078	0.0001	-0.0100
$4f_{5/2}5d_{5/2}(1)$	-0.1396	0.0235	-0.0004	-0.1396	$4f_{7/2}5f_{7/2}(1)$	-0.0030	-0.0028	-0.0012	-0.0024
$5p_{3/2}5d_{3/2}(1)$	0.6541	-0.1439	0.0008	0.6541	$4f_{5/2}5f_{7/2}(1)$	-0.0096	-0.0033	0.0004	-0.0097
$5p_{3/2}5d_{5/2}(1)$	-1.9529	0.4284	-0.0026	-1.9525	$4f_{5/2}5f_{5/2}(1)$	-0.0019	-0.0017	-0.0007	-0.0018
$5p_{1/2}5d_{3/2}(1)$	-1.3415	0.3112	-0.0025	-1.3413	$5p_{3/2}6p_{1/2}(1)$	-0.0838	-0.0087	0.0006	-0.0836
$5p_{3/2}6s_{1/2}(1)$	0.6495	0.0112	0.0012	0.6494	$5p_{3/2}6p_{3/2}(1)$	-0.0010	-0.0005	-0.0003	-0.0004
$5p_{1/2}6s_{1/2}(1)$	0.3359	0.0194	0.0015	0.3358	$5p_{1/2}6p_{1/2}(1)$	-0.0004	-0.0001	-0.0002	-0.0005
$4f_{7/2}6d_{5/2}(1)$	-0.1788	0.0158	-0.0004	-0.1788	$5p_{1/2}6p_{3/2}(1)$	-0.0704	-0.0069	0.0005	-0.0705
$4f_{5/2}6d_{3/2}(1)$	0.1474	-0.0191	0.0004	0.1474	$5p_{3/2}5f_{5/2}(1)$	0.0000	-0.0007	0.0001	-0.0002
$4f_{5/2}6d_{5/2}(1)$	-0.0392	0.0040	-0.0001	-0.0392	M2 uncoupled reduced matrix elements				
$5p_{3/2}6d_{3/2}(1)$	-0.0734	0.0469	-0.0004	-0.0734	$4f_{7/2}5d_{3/2}(2)$	-1.3949	0.6026	-0.0016	-2.7897
$5p_{3/2}6d_{5/2}(1)$	-0.2541	0.1310	-0.0005	-0.2542	$4f_{7/2}5d_{5/2}(2)$	-3.5300	0.5878	-0.0070	-7.0596
$5p_{1/2}6d_{3/2}(1)$	0.2239	-0.1583	0.0006	0.2240	$4f_{5/2}5d_{3/2}(2)$	-1.0256	-0.1313	-0.0026	-2.0512
$5p_{3/2}7s_{1/2}(1)$	0.2448	0.0404	0.0006	0.2448	$4f_{5/2}5d_{5/2}(2)$	0.0000	0.6400	0.0000	0.0000
$5p_{1/2}7s_{1/2}(1)$	0.1368	0.0485	0.0006	0.1368	$4f_{5/2}6s_{1/2}(2)$	0.0000	0.0328	0.0000	0.0000
E2 uncoupled reduced matrix elements					$4f_{7/2}6d_{3/2}(2)$	0.3700	0.1026	0.0009	0.7399
$4f_{5/2}6p_{1/2}(2)$	0.1004	0.0310	0.0006	0.2008	$4f_{7/2}6d_{5/2}(2)$	-0.9694	-0.2670	-0.0021	-1.9387
$4f_{7/2}6p_{3/2}(2)$	0.0957	0.0374	0.0006	0.1912	$4f_{5/2}6d_{3/2}(2)$	0.2785	0.0761	0.0008	0.5570
$4f_{5/2}6p_{3/2}(2)$	0.0330	0.0149	0.0004	0.0660	$4f_{5/2}6d_{5/2}(2)$	0.0000	0.0243	0.0000	0.0000
$4f_{7/2}5f_{5/2}(2)$	-0.1284	-0.0053	-0.0005	-0.2567	$4f_{5/2}7s_{1/2}(2)$	0.0000	-0.0016	0.0000	0.0000
$4f_{7/2}5f_{7/2}(2)$	0.3650	0.0152	0.0016	0.7298	$5p_{3/2}5d_{3/2}(2)$	0.0000	-0.0822	0.0001	0.0000
$4f_{5/2}5f_{7/2}(2)$	0.1186	0.0050	0.0007	0.2372	$5p_{3/2}5d_{5/2}(2)$	-8.6106	-0.9253	-0.0118	-17.2201
$4f_{5/2}5f_{5/2}(2)$	0.2952	0.0131	0.0016	0.5903	$5p_{1/2}5d_{3/2}(2)$	-1.0388	0.0503	-0.0020	-2.0778
$5p_{3/2}6p_{1/2}(2)$	-0.9641	-0.0580	-0.0011	-1.9280	$5p_{1/2}5d_{5/2}(2)$	3.3626	0.0738	0.0069	6.7245
$5p_{3/2}6p_{3/2}(2)$	0.8051	0.0456	0.0019	1.6100	$5p_{3/2}6d_{3/2}(2)$	0.0000	0.0149	0.0000	0.0000
$5p_{1/2}6p_{3/2}(2)$	0.5616	0.0304	0.0028	1.1229	$5p_{3/2}6d_{5/2}(2)$	-1.1202	-0.2533	-0.0024	-2.2410
$5p_{3/2}5f_{5/2}(2)$	-0.8417	0.0099	-0.0025	-1.6831	$5p_{1/2}6d_{3/2}(2)$	0.1733	-0.0453	0.0005	0.3465
$5p_{3/2}5f_{7/2}(2)$	2.0498	-0.0322	0.0065	4.0987	$5p_{1/2}6d_{5/2}(2)$	0.6154	0.4015	0.0007	1.2311
$5p_{1/2}5f_{5/2}(2)$	1.2693	-0.0109	0.0057	2.5381	$5p_{3/2}6s_{1/2}(2)$	2.5158	-0.0524	0.0046	5.0306
E3 uncoupled reduced matrix elements					$5p_{3/2}7s_{1/2}(2)$	0.9482	0.2018	0.0021	1.8961
$4f_{7/2}5d_{3/2}(3)$	-0.4924	0.2166	-0.0022	-1.5045	M3 uncoupled reduced matrix elements				
$4f_{7/2}5d_{5/2}(3)$	0.8611	-0.2686	0.0040	2.5986	$4f_{7/2}6p_{1/2}(3)$	0.4999	0.1308	0.0012	1.4994
$4f_{5/2}5d_{3/2}(3)$	0.6410	0.1112	0.0038	1.9253	$4f_{5/2}6p_{1/2}(3)$	0.0849	-0.0079	0.0005	0.2548
$4f_{5/2}5d_{5/2}(3)$	0.5277	0.4472	0.0032	1.5661	$4f_{7/2}6p_{3/2}(3)$	0.5558	0.1367	0.0033	1.6668
$4f_{7/2}6s_{1/2}(3)$	-0.4896	0.1822	-0.0028	-1.4805	$4f_{5/2}6p_{3/2}(3)$	0.0233	0.1142	0.0002	0.0700
$4f_{5/2}6s_{1/2}(3)$	-0.3952	0.1334	-0.0030	-1.1839	$4f_{7/2}5f_{5/2}(3)$	0.2870	0.2419	0.0011	0.8610
$4f_{7/2}6d_{3/2}(3)$	-0.0082	0.0024	0.0000	-0.0204	$4f_{7/2}5f_{7/2}(3)$	3.2481	1.2694	0.0142	9.7430
$4f_{7/2}6d_{5/2}(3)$	0.0039	-0.0056	-0.0002	0.0144	$4f_{5/2}5f_{7/2}(3)$	-0.2652	-0.2831	-0.0016	-0.7956
$4f_{5/2}6d_{3/2}(3)$	-0.0012	0.0272	0.0002	-0.0040	$4f_{5/2}5f_{5/2}(3)$	0.7670	0.1820	0.0044	2.3009
$4f_{5/2}6d_{5/2}(3)$	0.0118	-0.0422	-0.0003	0.0325	$5p_{3/2}6p_{3/2}(3)$	6.3906	0.6416	0.0148	19.1690
$4f_{7/2}7s_{1/2}(3)$	-0.1272	-0.0388	-0.0007	-0.3853	$5p_{3/2}5f_{7/2}(3)$	11.9084	3.4355	0.0379	35.7204
$4f_{5/2}7s_{1/2}(3)$	-0.1068	-0.0226	-0.0007	-0.3200	$5p_{3/2}5f_{5/2}(3)$	-0.5951	0.2886	-0.0019	-1.7850
$5p_{3/2}5d_{3/2}(3)$	-3.3615	-0.0278	-0.0140	-10.1499	$5p_{1/2}5f_{5/2}(3)$	1.0727	0.1715	0.0049	3.2186
$5p_{3/2}5d_{5/2}(3)$	2.8107	0.0209	0.0109	8.3961	$5p_{1/2}5f_{7/2}(3)$	-5.5355	-1.4489	-0.0265	-16.6036
$5p_{1/2}5d_{5/2}(3)$	2.6949	0.0913	0.0136	7.9958					
$5p_{3/2}6d_{3/2}(3)$	-1.0086	-0.2580	-0.0019	-3.0296					
$5p_{3/2}6d_{5/2}(3)$	-0.7451	-0.1976	-0.0027	-2.2331					
$5p_{1/2}6d_{5/2}(3)$	-0.4361	-0.7362	-0.0036	-1.3107					

the ratios became much larger (50–70%). The ratios of the second and first ($Z^{(2)}/Z^{(1)}$) orders are much smaller for the E2 transitions (1-5% for most of cases), except for the three $4f_j6p_{j'}(2)$ states when the ratios are about 30-50%. We find that second-order contributions for the E3 transitions became very large when the values of the reduced matrix elements became very small (see, for example, the case of the $4f_j6d_{j'}(3)$ states).

The magnetic-dipole matrix elements for the transitions between the two even-parity $4f_{5/2}6p_{3/2}(1)$ and $5p_{3/2}5f_{5/2}(1)$ excited states and the ground state have almost zero value of the $Z^{(1)}$ matrix elements (0.000038

TABLE VIII: Coupled reduced matrix elements $av(J)$ calculated in length L and velocity V forms for W VII.

$av(J)$	RMBPT1		RMBPT	
	L	V	L	V
E1 coupled reduced matrix elements				
$5p_{3/2}5d_{3/2}(1)$	-0.0575	-0.0438	-0.0425	-0.0415
$4f_{5/2}5d_{3/2}(1)$	-0.2666	-0.2042	-0.1699	-0.1733
$5p_{3/2}5d_{5/2}(1)$	0.9868	0.6759	0.7906	0.7580
$5p_{3/2}6s_{1/2}(1)$	-0.5759	-0.4466	-0.6192	-0.6067
$5p_{1/2}5d_{3/2}(1)$	2.3793	1.7154	1.8409	1.8047
$5p_{1/2}6s_{1/2}(1)$	0.2912	0.2364	0.3373	0.3325
$5p_{3/2}6d_{5/2}(1)$	-0.3954	-0.2743	-0.2289	-0.2215
E2 coupled reduced matrix elements				
$4f_{7/2}5f_{5/2}(2)$	0.0533	0.0424	0.0489	0.0472
$5p_{3/2}6p_{1/2}(2)$	-1.0186	-0.8136	-0.9019	-0.9016
$5p_{3/2}6p_{3/2}(2)$	-0.8229	-0.6667	-0.7323	-0.7250
$5p_{1/2}6p_{3/2}(2)$	-1.0182	-0.8348	-0.8969	-0.8769
$5p_{3/2}5f_{5/2}(2)$	-0.3916	-0.3216	-0.3248	-0.3194
$5p_{3/2}5f_{7/2}(2)$	-1.9787	-1.6232	-1.6891	-1.6602
$5p_{1/2}5f_{5/2}(2)$	1.2627	1.0403	1.1047	1.0794
E3 coupled reduced matrix elements				
$4f_{5/2}5d_{5/2}(3)$	0.6114	0.4354	0.6740	0.6672
$4f_{7/2}7s_{1/2}(3)$	0.0785	0.0635	0.0964	0.0968
$4f_{5/2}7s_{1/2}(3)$	0.0679	0.0548	0.0707	0.0708
$5p_{3/2}6d_{3/2}(3)$	-1.2033	-1.0747	-1.3670	-1.3208
$5p_{3/2}6d_{5/2}(3)$	-0.8543	-0.7651	-1.0008	-0.9614

and 0.000040, respectively). The non-zero values are due to relativistic contribution (see for detail Ref. [48]). The major contribution for these M1 matrix elements are from the $Z^{(2)}$ second-order RMBPT as was shown in Table VII. The ratio of the second and first $(Z^{(2)}/Z^{(1)})$ orders is very large (more than 30%) for four $4f_j5f_{j'}(1)$ matrix elements.

The magnetic-quadrupole matrix elements for the transitions between the two even-parity $4f_{5/2}6s_{1/2}(2)$ and $4f_{5/2}7s_{1/2}(2)$ excited states and the ground state are very small in the lowest order (0.000005 and 0.000002, respectively). The first-order contributions for the transitions from $4f_{5/2}5d_{5/2}(2)$, $4f_{5/2}6d_{5/2}(2)$, $5p_{3/2}5d_{3/2}(2)$, and $5p_{3/2}6d_{3/2}(2)$ to the ground state are equal to zero because the corresponding factor $(\kappa_a + \kappa_v)$, where κ_i is a relativistic angular momentum quantum number of a state i in Eq. (A.23) of Ref. [33] for $Z^{(1)}$ equals to zero for these transitions. The ratio of the second and first $(Z^{(2)}/Z^{(1)})$ orders for the other 14 transitions varies from 2% for the $5p_{1/2}5d_{5/2}(2)$ state up to 65% for the $5p_{1/2}6d_{5/2}(2)$ state.

The largest values of the ratio of the second and first $(Z^{(2)}/Z^{(1)})$ orders are about factors of 1–4 for the M3 matrix elements for the transitions between the three even-parity $4f_{5/2}5f_{7/2}(2)$, $4f_{7/2}5f_{7/2}(2)$, and $4f_{5/2}6p_{13/2}(2)$ excited states and the ground state. The $Z^{(2)}/Z^{(1)}$ ratios for the other 10 M3 transitions are about 10-40%.

In Table VIII, we present values of E1, E2, E3 *coupled* reduced matrix elements in length and velocity forms for the transitions considered in Table VII. Although we use an intermediate-coupling scheme, it is nevertheless convenient to label the physical states using the jj scheme. The first two columns in Table VIII show L and V values of *coupled* reduced matrix elements calculated without the second-order contribution. We can see huge of $L-V$ difference for some transitions. The second-order contribution dramatically decreases those $L-V$ difference up to 1%–4%. These small L–V differences arise because we start our RMBPT calculations using a non-local Dirac-Fock (DF) potential.

The E1, E2, E3, M2, M3, and M3 transition probabilities A_r (s^{-1}) for the transitions between the ground state and $4f_jnl_{j'}(J)$ and $5p_jnl_{j'}(J)$ states are obtained in terms of line strengths S (a.u.) and energies E (a.u.) as

$$\begin{aligned} A(EK) &= \frac{C^{(K)}\,[E]^{2K+1}}{(2J+1)}S(EK), \\ C^{(1)} &= 2.14200\times10^{10}, \\ C^{(2)} &= 5.70322\times10^{4}, \\ C^{(3)} &= 7.71311\times10^{-2} \\ A(MK) &= \frac{D^{(K)}\,[E]^{2K+1}}{(2J+1)}S(MK), \\ D^{(1)} &= 2.85161\times10^{5}, \\ D^{(2)} &= 7.59260\times10^{-1}, \\ D^{(3)} &= 1.02683\times10^{-6}, \end{aligned} \tag{2}$$

It should be noted that the line strengths $S(E1)$, $S(E2)$, $S(E1)$, $S(E3)$, $S(M1)$, $S(M2)$, and $S(M3)$ are obtained as a square of *coupled* E1, E2, E3, M2, M3, and M3 matrix elements. The E1, E2, E3, M2, M3, M2, and M3 *coupled* matrix elements are evaluated using an intermediate-coupling scheme (see, [1, 33, 35, 36] for detail). Results of our calculation are given in Table IX.

In Table IX, we present wavelengths (in Å) and radiative rates (A_r) for the electric-multipole (E1, E2, and E3) and magnetic-multipole (M1, M2, and M3) transitions from $4fnl$ and $5pnl$ hole-particle states to the ground state in Er-like W^{6+} ion. We list available NIST [15] wavelength data in the column labeled 'NIST' in Table IX. We also use these data to evaluate transition rates given in columns 'RMBPT1' and 'RMBPT'. We did not find experimental energy values for some of the levels presented in Table V. We put RMBPT values from Table V in such cases and labelled them with asterisk in the column 'NIST'of Table IX.

Radiative rates are calculated in the first-order RMBPT1 and the second-order RMBPT. We can see substantial difference between results given in columns with the headings RMBPT1 and RMBPT of Table IX. This difference gives exact value of the correlation from second-order contribution. The ratios of transition rates A_r^{E1}/A_r^{E2} and A_r^{E2}/A_r^{M1} evaluated for E1, E2, and M1 transitions are equal to 10^3–10^6 and 10–100, respectively. The smallest value of transition rates is for the M3 transition (10^{-7}–10^{-2} s^{-1}). The values of transition rates

TABLE IX: Wavelengths (λ in Å) and radiative rates (A_r in s^{-1}) for E1, E2, E3, M1, M2, and M3 transitions from $[4f5d + 5p5d + 4f6d + 5p6d + 4f6s + 5p6s + 4f7s + 5p7s]$ and $[4f6p + 5p6p + 4f5f + 5p5f]$ excited states to the ground state in W VII. Asterisk designates RMBPT values for those transitions which levels are not included by NIST [15]. Numbers in brackets represent powers of 10.

	λ (Å)	Transition rate A_r (s^{-1})			λ (Å)	Transition rate A_r (s^{-1})	
$av(J)$	NIST[15]	RMBPT1	RMBPT	$av(J)$	NIST[15]	RMBPT1	RMBPT
E1 transitions				M1 transitions			
$5p_{3/2}5d_{3/2}(1)$	313.573	7.24[07]	3.95[07]	$4f_{5/2}6p_{3/2}(1)$	185.562	2.04[-3]	1.17[1]
$4f_{7/2}5d_{5/2}(1)$	302.272	4.23[06]	6.90[06]	$4f_{7/2}5f_{5/2}(1)$	161.732*	1.92[2]	7.73[2]
$4f_{5/2}5d_{3/2}(1)$	294.376	1.88[09]	7.64[08]	$4f_{7/2}5f_{7/2}(1)$	159.596	2.88[1]	5.55[1]
$4f_{5/2}5d_{5/2}(1)$	289.526	9.44[06]	2.95[07]	$4f_{5/2}5f_{7/2}(1)$	155.647	2.10[2]	4.77[2]
$5p_{3/2}5d_{5/2}(1)$	261.387	3.68[10]	2.36[10]	$4f_{5/2}5f_{5/2}(1)$	155.308	3.83[1]	3.30[1]
$5p_{3/2}6s_{1/2}(1)$	223.846	2.00[10]	2.31[10]	$5p_{3/2}6p_{1/2}(1)$	193.396	7.53[3]	9.39[3]
$5p_{1/2}5d_{3/2}(1)$	216.219	3.78[11]	2.26[11]	$5p_{3/2}6p_{3/2}(1)$	181.863	6.68[2]	7.62[2]
$5p_{1/2}6s_{1/2}(1)$	188.159	8.60[09]	1.15[10]	$5p_{1/2}6p_{1/2}(1)$	164.226*	3.47[0]	2.37[0]
$5p_{3/2}6d_{3/2}(1)$	154.448	1.40[08]	1.16[08]	$5p_{1/2}6p_{3/2}(1)$	158.486*	1.22[4]	1.48[4]
$5p_{3/2}6d_{5/2}(1)$	151.889	3.01[10]	1.01[10]	$5p_{3/2}5f_{5/2}(1)$	156.657*	1.66[2]	2.27[2]
$5p_{3/2}7s_{1/2}(1)$	153.848	8.71[09]	1.23[10]	M2 transitions			
$4f_{7/2}6d_{5/2}(1)$	147.025	1.28[10]	9.41[09]	$4f_{7/2}5d_{3/2}(2)$	321.088	4.88[0]	1.65[-3]
$4f_{5/2}6d_{3/2}(1)$	150.203	1.17[10]	8.59[09]	$4f_{7/2}5d_{5/2}(2)$	304.860	9.60[0]	1.32[0]
$4f_{5/2}6d_{5/2}(1)$	150.275	1.69[08]	1.83[08]	$4f_{5/2}5d_{3/2}(2)$	295.986	2.64[0]	6.93[-1]
$5p_{1/2}6d_{3/2}(1)$	134.959	2.91[10]	5.20[09]	$4f_{5/2}5d_{5/2}(2)$	287.051	7.95[-2]	1.22[0]
$5p_{1/2}7s_{1/2}(1)$	130.416	3.42[09]	7.92[09]	$4f_{5/2}6s_{1/2}(2)$	219.990	3.40[-5]	6.41[-3]
E2 transitions				$4f_{7/2}6d_{3/2}(2)$	157.389*	5.65[-4]	9.65[-4]
$4f_{5/2}6p_{1/2}(2)$	192.606	2.65[3]	3.36[3]	$4f_{7/2}6d_{5/2}(2)$	154.188	1.13[1]	1.69[1]
$4f_{7/2}6p_{3/2}(2)$	188.170	1.66[4]	2.56[4]	$4f_{5/2}6d_{3/2}(2)$	153.172*	1.43[0]	1.85[0]
$4f_{5/2}6p_{3/2}(2)$	183.945	1.09[3]	2.04[3]	$4f_{5/2}6d_{5/2}(2)$	150.781	7.02[-4]	2.19[-2]
$4f_{7/2}5f_{5/2}(2)$	159.738	6.11[3]	5.16[3]	$4f_{5/2}7s_{1/2}(2)$	144.248	4.93[-5]	1.66[-3]
$4f_{7/2}5f_{7/2}(2)$	158.740	2.96[5]	2.50[5]	$5p_{3/2}5d_{3/2}(2)$	298.492	4.78[1]	2.30[1]
$4f_{5/2}5f_{7/2}(2)$	154.692	8.91[4]	7.60[4]	$5p_{3/2}5d_{5/2}(2)$	291.286	6.20[1]	3.32[1]
$4f_{5/2}5f_{5/2}(2)$	154.821	1.97[5]	1.69[5]	$5p_{1/2}5d_{3/2}(2)$	239.209*	1.16[1]	6.00[0]
$5p_{3/2}6p_{1/2}(2)$	187.116	1.01[6]	7.94[5]	$5p_{1/2}5d_{5/2}(2)$	225.613	3.08[1]	9.56[0]
$5p_{3/2}6p_{3/2}(2)$	180.940	7.82[5]	6.19[5]	$5p_{3/2}6d_{3/2}(2)$	232.146	1.70[1]	8.85[0]
$5p_{1/2}6p_{3/2}(2)$	158.126	2.35[6]	1.82[6]	$5p_{3/2}6d_{5/2}(2)$	152.917	1.29[0]	1.21[0]
$5p_{3/2}5f_{5/2}(2)$	159.251*	3.35[5]	2.31[5]	$5p_{1/2}6d_{3/2}(2)$	151.439*	1.03[1]	9.06[0]
$5p_{3/2}5f_{7/2}(2)$	153.995*	1.01[7]	7.38[6]	$5p_{1/2}6d_{5/2}(2)$	147.286	1.95[1]	2.47[1]
$5p_{1/2}5f_{5/2}(2)$	144.846*	5.60[6]	4.29[6]	$5p_{3/2}6s_{1/2}(2)$	134.735*	1.14[0]	2.43[-1]
E3 transitions				$5p_{3/2}7s_{1/2}(2)$	134.189*	6.78[0]	2.57[1]
$4f_{7/2}5d_{3/2}(3)$	311.825	1.64[-2]	8.15[-3]	M3 transitions			
$4f_{7/2}5d_{5/2}(3)$	300.214	1.24[-1]	3.85[-2]	$4f_{7/2}6p_{1/2}(3)$	194.977	1.71[-5]	3.72[-5]
$4f_{5/2}5d_{3/2}(3)$	291.466	1.48[-1]	1.39[-2]	$4f_{5/2}6p_{1/2}(3)$	188.505	5.67[-8]	7.86[-7]
$4f_{5/2}5d_{5/2}(3)$	284.414	1.12[-1]	1.36[-1]	$4f_{7/2}6p_{3/2}(3)$	186.973	2.01[-5]	3.90[-5]
$4f_{7/2}6s_{1/2}(3)$	228.297	3.19[-1]	6.86[-4]	$4f_{5/2}6p_{3/2}(3)$	185.485	2.33[-7]	5.42[-6]
$4f_{5/2}6s_{1/2}(3)$	219.674	3.18[-1]	5.40[-3]	$4f_{7/2}5f_{5/2}(3)$	159.474	1.45[-3]	4.06[-3]
$4f_{7/2}6d_{3/2}(3)$	154.812	3.40[-2]	3.60[-2]	$4f_{7/2}5f_{7/2}(3)$	158.957	9.96[-4]	2.37[-3]
$4f_{7/2}6d_{5/2}(3)$	153.926	1.08[-1]	1.97[-1]	$4f_{5/2}5f_{7/2}(3)$	155.312	4.25[-5]	2.73[-5]
$4f_{5/2}6d_{3/2}(3)$	150.479	7.03[-2]	3.81[-1]	$4f_{5/2}5f_{5/2}(3)$	154.638	1.43[-4]	4.02[-4]
$4f_{5/2}6d_{5/2}(3)$	149.837	2.37[-2]	4.40[-1]	$5p_{3/2}6p_{3/2}(3)$	180.640	4.43[-3]	6.03[-3]
$4f_{7/2}7s_{1/2}(3)$	147.894	1.79[-1]	2.70[-1]	$5p_{3/2}5f_{7/2}(3)$	157.466*	3.04[-2]	6.49[-2]
$4f_{5/2}7s_{1/2}(3)$	144.203	1.60[-1]	1.73[-1]	$5p_{3/2}5f_{5/2}(3)$	156.797*	5.24[-3]	8.89[-3]
$5p_{3/2}5d_{3/2}(3)$	298.355	1.48[0]	4.02[0]	$5p_{1/2}5f_{5/2}(3)$	136.355*	1.50[-3]	2.58[-3]
$5p_{3/2}5d_{5/2}(3)$	282.397	3.20[0]	4.18[0]	$5p_{1/2}5f_{7/2}(3)$	131.823*	2.05[-2]	3.74[-2]
$5p_{1/2}5d_{5/2}(3)$	230.386*	1.12[1]	1.67[1]				
$5p_{3/2}6d_{3/2}(3)$	153.734	3.20[1]	6.83[1]				
$5p_{3/2}6d_{5/2}(3)$	152.401	1.72[1]	3.78[1]				
$5p_{1/2}6d_{5/2}(3)$	133.972*	2.06[1]	1.74[2]				

TABLE X: Multipole core polarizabilities $\alpha^{Ek}_{\rm core}$, calculated using DF and RPA approximation (a.u) in Er-like W^{6+} ion.

	α^{E1}	α^{E2}	α^{E3}
RPA	2.05	2.58	9.06
DF	2.50	2.31	7.35

change inside the complex of states with fixed J by three-four orders of magnitude. As a result, the values of the transition rates given in Table IX vary from 10^{-7} s^{-1} for the M3 transition up to 10^{10} s^{-1} for the E1 transition.

V. CORE MULTIPOLE POLARIZABILITIES IN ER-LIKE TUNGSTEN

The core multipole polarizability $\alpha^{Ek}_{\rm core}$ is evaluated here in the random-phase approximation (RPA) [49] and DF approximation. The $\alpha^{Ek}_{\rm core}$ contribution is calculated using the sum-over-state approach

$$\alpha^{Ek}_{\rm core} = \frac{2}{2k+1}\sum_{n,a}\frac{|\langle nl_j\|r^k C_{kq}\|al'_{j'}\rangle|^2}{E_{nlj}-E_{al'j'}}, \qquad (3)$$

where $C_{kq}(\hat{r})$ is a normalized spherical harmonic and where $al'j'$ include all core states in Er-like ions from the $1s_{1/2}$ up to $5p_j$ states, nl_j includes all valence states above core for k = 1, 2, and 3, respectively [50]. The reduced matrix elements in the above sum are evaluated using DF and RPA approximation for states with n up to n =50.

In Table X, we present multipole core polarizabilities $\alpha^{Ek}_{\rm core}$, calculated using DF and RPA approximation in Er-like W^{6+} ion . The correlation contributions estimated as the difference between the RPA and DF values are about 20% for the $\alpha^{Ek}_{\rm core}$ with k = 1 and 3, while only 10% for the $\alpha^{Ek}_{\rm core}$ with k = 2.

VI. UNCERTAINTY ESTIMATES AND CONCLUSION

Comparison of the RMBPT1 and RMBPT energies and transition rates presented in Tables V and IX gives us the first rough estimation of uncertainties of our results. In particular, the difference in the RMBPT1 and RMBPT is about 8% for energies, and is about 50% for the largest values of transitions rates A_r and a factor of 2 for the smallest values of A_r. The difference between the RMBPT1 and RMBPT values is the second-order correction. The third-order corrections for the energies and transition rates were evaluated for monovalent atomic systems (see, for example, Refs. [51–53]). The difference between the RMBPTI3 and RMBPT2 energies was about 2-3% for Ba II, Sr II, and Hg II ions. We also found 2-3% difference between our RMBPT energies and NIST values given in Table V. Only 8 levels among 100 levels deviate from NIST values for more than 3%. Therefore, we estimate uncertainties of 3% for the other 32 levels not identified in NIST compilation [15]. We already mentioned above that in addition, the energies and wavelengths in W VII ion were evaluated using the HULLAC and COWAN codes. There are only three among 16 cases when the difference is larger than 2%.

Also, to check accuracy of our calculations for transition rates, we evaluate the E1, E2, E3 *coupled* reduced matrix elements in length and velocity forms. Results given in Table VIII show that the $L-V$ difference for the RMBPT1 values is about 20-30%, while the $L-V$ difference for the RMBPT values is about 1-4%. So, we estimate our accuracy for transition rates as about 10-20% for the largest values of A_r and about 20-50% for the smallest values of A_r.

The estimation of the accuracy our RPA results for the core multipole polarizabilities (which is about 10-20%) is based on recent review of theory and applications of atomic and ionic polarizabilities [54].

We have presented a systematic second-order relativistic MBPT study of excitation energies, reduced matrix elements, and transition rates for multipole transitions in Er-like tungsten ion. Our retarded multipole matrix elements include correlation corrections from Coulomb and Breit interactions. We determine energies of the $4f_j5d_{j'}(J)$, $5p_j5d_{j'}(J)$ $4f_j6d_{j'}(J)$, $5p_j6d_{j'}(J)$, $4f_j6p_{j'}(J)$, $5p_j6p_{j'}(J)$, $4f_j5f_{j'}(J)$, $5p_j5f_{j'}(J)$ $4f_j6s_{1/2}(J)$, $5p_j6s_{1/2}(J)$, $4f_j7s_{1/2}(J)$, and $5p_j7s_{1/2}(J)$ excited states. Wavelengths and transition rates were evaluated for the 90 multipole matrix elements for transitions from excited states into the ground states. Core multipole polarizabilities in Er-like W^{6+} ion are calculated in DF and RPA approximation. Our RMBPT results presented in this paper are the first *ab initio* calculations of energies and transition rates in Er-like tungsten. The comparison with results with other codes as well as with available experimental data is discussed. These data are important for diagnostics of low-ionized tungsten plasma for fusion application.

Acknowledgments

This research was sponsored by DOE under the OFES grant DE-FG02-08ER54951 and in part under the NNSA CA DE-FC52-06NA27588.

[1] U. I. Safronova and M. S. Safronova, Phys. Rev. A **79**, 032511 (2009).

[2] B. W. Bryant, J. Opt. Soc. Am. **55**, 771 (1965).

[3] J. Sugar and V. Kaufman, J. Opt. Soc. Am. **62**, 562 (1972).
[4] J. Sugar and V. Kaufman, J. Opt. Soc. Am. **64**, 1656 (1974).
[5] V. Kaufman and J. Sugar, J. Opt. Soc. Am. **65**, 302 (1975).
[6] J. Sugar and V. Kaufman, Phys. Rev. A **12**, 994 (1975).
[7] U. I. Safronova and A. S. Safronova, J. Phys. B **43**, 074026 (2010).
[8] U. I. Safronova and A. S. Safronova, Can. J. Phys. **87**, 83 (2009).
[9] U. I. Safronova, A. S. Safronova, and W. R. Johnson, J. Phys. B **43**, 144001 (2010).
[10] U. I. Safronova, A. S. Safronova, and P. Beiersdorfer, At. Data Nucl. Data Tab. **95**, 751 (2009).
[11] U. I. Safronova, A. S. Safronova, and P. Beiersdorfer, J. Phys. B **42**, 165010 (2009).
[12] U. I. Safronova, A. S. Safronova, P. Beiersdorfer, and W. R. Johnson, J. Phys. B **44**, 035005 (2010).
[13] A. V. Loginov and V. I. Tuchkin, Opt. Spectr. **90**, 631 (2001).
[14] G. P. Anisimova, A. V. Loginov, and V. I. Tuchkin, Opt. Spectr. **90**, 315 (2001).
[15] A. E. Kramida and T. Shirai, At. Data and Nucl. Data Tables **95**, 305 (2009).
[16] J. Clementson, P. Beiersdorfer, E. W. Magee, H. S. McLean, and R. D. Wood, J. Phys. B **43**, 144009 (2010).
[17] J. Clementson, P. Beiersdorfer, and M. F. Gu, Phys. Rev. A **81**, 012505 (2010).
[18] J. Clementson, P. Beiersdorfer, G. V. Brown, and M. F. Gu, Phys. Scr. **81**, 015301 (2010).
[19] C. S. Harte, C. Suzuki, T. Kato, H. A. Sakaue, D. Kato, K. Sato, N. Tamura, S. Sudo, R. D'Arcy, and E. Sokell, J. Phys. B: At. Mol. Opt. Phys. **43**, 205004 (2010).
[20] J. Clementson and P. Beiersdorfer, Phys. Rev. A **81**, 052509 (2010).
[21] P. Beiersdorfer, J. Clementson, J. Dunn, M. F. Gu, K. Morris, Y. Podpaly, E. Wang, M. Bitter, R. Feder, K. Hill, et al., J. Phys. B **43**, 144008 (2010).
[22] J. Clementson, P. Beiersdorfer, A. L. Roquemore, C. H. Skinner, D. K. Manseld, K. Hartzfeld, and J. K. Lepson, Rev. Scientific Instr. **81**, 10E326 (2010).
[23] M. Reinke, P. Beiersdorfer, N. T. Howard, E. W. Magee, Y. Podpaly, J. E. Rice, and J. L. Terry, Rev. Scientific Instr. **81**, 10D736 (2010).
[24] J. Yanagibayashi, T. Nakano, A. Iwamae, H. Kubo, M. Hasuo, and K. Itami, J. Phys. B **43**, 144013 (2010).
[25] C. Biedermann, R. Radtke, R. Seidel, and E. Behar, J. Phys. Conf. Series **163**, 012034 (2009).
[26] C. Biedermann, R. Radtke, R. Seidel, and T. Pütterich, Phys. Scr. **T134**, 014026 (2009).
[27] J. Reader, Physica Scripta **134**, 014023 (2009).
[28] Y. Podpaly, J. Clementson, P. Beiersdorfer, J. Williamson, G. V. Brown, and M. F. Gu, Phys. Rev. A **80**, 052504 (2009).
[29] J. Clementson, P. Beiersdorfer, M. F. Gu, H. S. McLean, and R. D. Wood, J. Phys. Conf. Series **130**, 012004 (2008).
[30] R. D. Cowan, *The Theory of Atomic Structure and Spectra* (University of California Press, Berkeley, 1981).
[31] U. I. Safronova, W. R. Johnson, and J. Albritton, Phys. Rev. A **62**, 052505 (2000).
[32] U. I. Safronova, C. Namba, I. Murakami, W. R. Johnson, and M. Safronova, Phys. Rev. A **64**, 012517 (2001).
[33] S. M. Hamasha, A. S. Shlyaptseva, and U. I. Safronova, Can. J. Phys. **82**, 331 (2004).
[34] U. I. Safronova, T. E. Cowan, and W. R. Johnson, Can. J. Phys. **83**, 813 (2005).
[35] U. Safronova, A. S. Safronova, S. M. Hamasha, and P. Beiersdorfer, At. Data Nucl. Data Tabl. **92**, 47 (2006).
[36] U. Safronova, A. S. Safronova, and P. Beiersdorfer, J. Phys. B **39**, 4491 (2006).
[37] U. I. Safronova, R. Bista, R. Bruch, and H. Merabet, Can. J. Phys. **86**, 131 (2008).
[38] U. Safronova, T. E. Cowan, and A. S. Safronova, J. Phys. B **38**, 2741 (2005).
[39] U. I. Safronova, A. S. Safronova, and P. Beiersdorfer, J. Phys. B **40**, 955 (2007).
[40] U. I. Safronova, A. S. Safronova, and P. Beiersdorfer, Phys. Rev. A **77**, 032506 (2008).
[41] W. R. Johnson, S. A. Blundell, and J. Sapirstein, Phys. Rev. A **37**, 2764 (1988).
[42] M. H. Chen, K. T. Cheng, and W. R. Johnson, Phys. Rev. A **47**, 3692 (1993).
[43] L. W. Fullerton and G. A. Rinker, Jr., Phys. Rev. A **13**, 1283 (1976).
[44] P. J. Mohr, Ann. Phys. (N.Y.) **88**, 26 (1974).
[45] P. J. Mohr, Ann. Phys. (N.Y.) **88**, 52 (1974).
[46] P. J. Mohr, Phys. Rev. Lett. **34**, 1050 (1975).
[47] U. I. Safronova, W. R. Johnson, A. Shlyaptseva, and S. Hamasha, Phys. Rev. A **67**, 052507 (2003).
[48] U. I. Safronova, W. R. Johnson, and A. Derevianko, Phys. Scr. **60**, 46 (1999).
[49] W. R. Johnson, D. Kolb, and K.-N. Huang, At. Data Nucl. Data Tables **28**, 333 (1983).
[50] W. R. Johnson, D. R. Plante, and J. Sapirstein, Adv. Atom. Mol. Opt. Phys. **35**, 255 (1995).
[51] U. I. Safronova, Phys. Rev. A **81**, 052506 (2010).
[52] U. I. Safronova, Phys. Rev. A **82**, 022504 (2010).
[53] U. I. Safronova and W. R. Johnson, Phys. Rev. A **69**, 052511 (2004).
[54] J. Mitroy, M. S. Safronova, and C. W. Clark, J. Phys. B **43**, 202001 (2010).